Master of Medicine

Evaluation of novel 4D scaffold for bone regeneration in a rabbit model of an iliac crest undercut defects

The Graduate School
of the University of Ulsan

Department of Medicine
Min Jae Kim

Evaluation of novel 4D scaffold for bone regeneration in a rabbit model of an iliac crest undercut defects

Supervisor: Bu-Kyu Lee DDS MSD PhD

A dissertation

Submitted to
Graduate School of University of Ulsan
In partial Fulfillment of the Requirements
for the Degree of

Master of Medicine

By

Min Jae Kim

Department of Medicine
University of Ulsan, Korea
February 2024

Evaluation of novel 4D scaffold for bone regeneration in a rabbit model of an iliac crest undercut defects

This certifies that the dissertation/master thesis
of Min Jae Kim is approved.

Changmo Hwang
Committee Chair Dr.

Bu-Kyu Lee
Committee Member Dr.

Jee-Ho Lee
Committee Member Dr.

Department of Medicine
University of Ulsan, Korea
February 2024

English abstract

Evaluation of novel 4D scaffold for bone regeneration in a rabbit model of an iliac crest undercut defects

Min Jae Kim, D.D.S

Directed by Bu-Kyu Lee, D.D.S., M.S.D., PhD

Department of Dentistry, Graduate school of Medicine, University of Ulsan

Introduction:

In the craniomaxillofacial area, bone defects may result from various causes, including tumors, cysts, trauma, bone necrosis, and other factors. Therefore, reconstruction is necessary to resolve the disability caused by bone defects. Among the various defects, bone defects in the form of undercuts with a narrow entrance are commonly observed, and these are difficult to reconstruct using conventional 3D printing technology. The graft material, using customized 4D printing technology in this study, utilized the property of hydration gel to absorb surrounding water and expand, enhancing the filling of undercut defects. This study aims to determine the suitability of this 4D printing bone graft material for the craniomaxillofacial region in an in-vivo environment.

Materials and Methods:

A total of fifteen New Zealand white rabbits underwent trapezoidal undercut defect formation, treated with three groups: defect group, 3D scaffold group, and 4D scaffold group. After 6 and 12 weeks, each rabbit was sacrificed, and samples were prepared. Subsequently, the bone generation, expansion capability, and maintenance of the initial structure were assessed through CT and histological analysis.

Results:

The study observed varied complications among the cases, including fractures (23%), and dislocations (23%). In normal healing cases, contrary to expectations, a lot of bone regeneration occurred in the defect area. However, this allowed us to confirm the location of the scaffold and evaluate its bone formation ability, expansion ability, and maintenance of the initial structure. Bone generation analysis at 6weeks demonstrated significant differences in bone generation between the 4D scaffold group (29.16%) and the 3D scaffold group (7.82%). The confirmation of the 4D scaffold's expansion capability is evidenced by a larger shaded area compared to the 3D scaffold group at 6weeks. Furthermore, the 4D scaffold group exhibited superior maintenance of bone height (83% to 87%) compared to other groups at 12weeks. Histopathological assessments indicated enhanced bone formation and reduced inflammatory responses in the 4D scaffold group.

Conclusion:

This study signifies the potential of 4D printing technology in scaffold design for craniomaxillofacial bone defect reconstruction. Despite the experimental model's limitations, characterized by an accelerated bone formation capability, the 4D scaffold represent superior bone generation, expansion capability, and maintenance of structure. Histological examinations affirmed the scaffold's biocompatibility and efficacy in bone generation. While further research is essential, these findings underscore the promise of 4D printing in addressing complex bone defects.

Keywords: 4D printing technology, craniomaxillofacial reconstruction, bone defect

Contents

List of tables

List of figures

Introduction

In the craniomaxillofacial area, bone defects may result from various causes, including tumors, cysts, trauma, bone necrosis, and other factors. Therefore, reconstruction is necessary to resolve the disability caused by bone defects. A scaffold for bone reconstruction is one of the areas being researched in the field of bone tissue engineering, with the goal of ideally regenerating deficient bone tissue. These scaffolds are designed to be transplanted into the defect site, providing a stable three-dimensional (3D) space for bone tissue growth while also being developed for the purpose of delivering drugs or cells to the defect site. Therefore, scaffolds need to provide sufficient interconnected porosity for the influx and growth or storage of cells or tissues. Early scaffold development aimed at implementing porous structures for gas foaming [1-3] or salt leaching [4-6] methodologies to evaluate the potential use of such porous structures as scaffolds. However, with the rapid advancement of additive manufacturing (AM) technology in recent years, allowing for the adjustment of variables that can impact bone regeneration in scaffold development, there is a more active pursuit of research on the development of advanced functional scaffolds [7-10].

Meanwhile, the use of AM technology in scaffold development has enabled the creation of customized scaffolds for arbitrary 3D shapes. With the possibility of customized scaffold fabrication, there is not only progress in tailored restoration for defect shapes [10] but also a growing realization of the potential for customized regeneration of the functionality of the defect site. According to previous studies, the experimental verification suggests that as the shape compatibility between the scaffold and the defect bone tissue increases, the efficacy of bone regeneration can be significantly improved. Therefore, the development of customized scaffolds for defect bone tissue has become a crucial aspect, along with the technology for producing defect-shaped scaffolds using AM and its effectiveness evaluation [10-12]. However, most of the reported scaffolds to date have been somewhat neglectful of the morphological aspects of bone defects that occur in actual clinical situations. Many developed scaffolds have focused on improving bone regeneration efficacy and mechanical properties, with an

emphasis on validation for these aspects, often overlooking real clinical scenarios. Bone defects can arise from various causes, including conditions like avascular necrosis, where vascular insufficiency is a contributing factor. Since trabecular bone contains essential elements for regeneration and activity, such as nerves and blood vessels, if vascular insufficiency occurs, necrosis may initiate from the trabecular bone. Consequently, if necrosis starts from the trabecular bone, more extensive necrosis is likely to progress than the surrounding cortical bone, increasing the susceptibility to fractures from external impacts or loads. In such cases, an undercut defect, where the internal defect size is larger than the external defect size, may occur, making the application of most existing 3D customized scaffolds impractical.

As an alternative to this, recent developments in scaffolds using 4D printing technology with smart materials have been introduced, presenting various customized scaffolds. In the context of 4D printing, it refers to the latest manufacturing technology where a 3D structure responds to external environmental factors, leading to changes in its shape and functionality over time. This technology has demonstrated its potential in the field of bone tissue engineering as a scaffold with customized functionality. For instance, Xie et al. developed a scaffold using shape-memory effect thermoplastic polyurethane (TPU) that exhibits shape memory effects at body temperature [13]. Similarly, Wang et al. developed a scaffold using TCP/P (DLLA-TMC) material with shape memory effects at body temperature through an AM process [14]. These studies propose the potential utility of scaffolds for critical defect reconstruction with arbitrary shapes. However, the use of scaffolds based on 4D printing technology is still in the early stages of research and development, requiring further studies for clinical application. Apart from examples of applications in cartilaginous areas such as trachea support devices [15], the utilization of these scaffolds for bone regeneration is limited due to constraints related to material functionality and mechanical properties. Additionally, a common and significant hurdle for the clinical application of developed scaffolds is the safety verification of the materials used. Specifically, for 4D scaffolds, the validation of efficacy and safety over an extended period of implantation in the body is essential. However, this process demands considerable time and resources.

Therefore, the most practical approach to lowering the hurdles for clinical application is to utilize certified materials currently in use.

In this study, we developed a 4D scaffold using hyaluronic acid capable of shape-matching behavior through wetting expansion. According to previous reports, hyaluronic acid exhibits a very high wetting expansion ratio [16-18], and its efficacy and safety have been verified, leading to its use in various fields such as fillers [19, 20], anti-adhesive agents [21, 22], and cosmetics [23, 24]. Therefore, in this study, we propose a shape-matching 4D scaffold for customized reconstruction of bone defects based on the wetting expansion behavior of commercially available hyaluronic acid fillers. To minimize the possibility of filler leakage into external tissues when injecting only hyaluronic acid filler, we suggest a polycaprolactone (PCL) structure with an expansible, growth-friendly membrane pattern according to the wetting expansion behavior of hyaluronic acid. To evaluate the histological efficacy of the proposed shape-matching 4D scaffold, we also introduce a novel undercut defect model. Through histological evaluation using the undercut defect model, we confirmed the potential utility of the proposed 4D scaffold for bone regeneration as a medical device.

Materials and Methods

1. The in vivo animal model

All animal experiments were performed in compliance with the relevant guidelines and regulations of the Animal Ethics Committee of Asan Medical Center, which is approved for animal research management by the Ministry of Food and Drug Safety of South Korea (approval number 2022-12-160). Fifteen New Zealand white rabbits (2.5-3 kg) were used in the study. The experiment was performed on the both rabbit iliac crest, which has a sufficient bone thickness of 4 to 5 mm, enabling the creating trapezoidal undercut defects (top side: 5mm, height: 10mm, bottom side: 12mm). A total 16 rabbits were involved in the experiment. Each rabbit received treatment on both sides of the iliac bone. Two models were established: a short-term model and a long-term model. In the short-term

models, 8 rabbits were sacrificed at 6 weeks, while in the long-term models, the other 8 rabbits were sacrificed at 12 weeks. In each model, iliac defects were treated with four groups: the untreated group (n=1), the defect group (n=5), the 3D scaffold group (n=5), and the 4D scaffold group (n=5) (Figure 1, 2, 3).

2. The scaffold system

A. Materials

The hyaluronic acid (Restylane® Volyme™, Galderma, Switzerland) and PCL (MW: 37,000, Polysciences Inc., Warrington, PA, USA) used for the fabrication of the 4D scaffold were purchased. The hyaluronic acid used in this study has been certified by the U.S. FDA and European CE. For PCL, it was melted sufficiently at 85℃ and then conveyed to the screw pump with compressed air at 350 kPa. Components constituting the 4D scaffold were printed through 100μm and 400μm precision nozzles using a screw pump at 15 rpm. The AM system used for the fabrication of the 4D scaffold in this study utilized equipment reported in previous research [11, 12].

B. Scaffolds

In the case of 4D scaffold, upon the injection of the hyaluronic acid, the hyaluronic acid undergoes swelling while retaining surrounding moisture, subsequently inducing the expansion of the auxetic membrane. In this study, the centrally positioned triangular area of the auxetic membrane expanded and rotated forward, subsequently filling the trapezoidal defect. Moreover, within the 4D scaffold, the membrane was structured to facilitate and guide the expansion of the 4D scaffold. (Figure 4).

3. Surgical procedure

A. Direct approach & subperiosteal dissection

After removing the hair from both areas, povidone was applied to the skin. The iliac crests

on both sides are marked on the skin with a marking pen with the land mark of anterosuperior iliac supine (ASIS). Anesthesia was induced by intraperitoneal administration of zoletil and xylazine (at doses of 15 mg/kg and 3.5 mg/kg, respectively). In the middle part of the iliac crests, we design an incision of about 8-10cm from the front to the back. Following the design, we make an incision up to the periosteum with blade 15 and exfoliate. We thoroughly stop the bleeding site using hemostatic forceps. We complete subperiosteal dissection on the surfaces of the iliac crest is sufficiently performed, and secures enough space to perform osteotomy (Figure 5a).

B. Ostectomy

We designed the trapezoidal osteotomy line using a ruler (top side: 5mm, height: 10mm, bottom side: 12mm). We made a trapezoidal defect using saw and drill. In the 3D group, a 3D scaffold was applied to the defect. In the 4D group, 4D scaffolds were applied along with hyaluronic acid to the defect area. The periosteum was sutured using black silk, followed by the layer-by-layer closure of the fascia and skin using Nylon (Figure 5b-h).

C. Management after surgery

The rabbits were kept in a temperature-controlled environment with a 12-hour light/12-hour dark cycle, and they had free access to food and water. For three days after surgery, dressing was done by povidone, and analgesics and antibiotics were administered. The surgical site was palpated to determine if there was any abnormality.

D. Sacrifice

The short-term model and long-term models were sacrificed at 6 weeks, and 12weeks. Euthanasia was performed using 5 mL of KCl into the ear vein. And, the specimen was collected along with the muscle to prevent damage to the scaffold.

4. Ex vivo micro-CT imaging analysis

Ex vivo micro-CT imaging was carried out using an ex vivo animal scanner (SkyScan 1172; Bruker-microCT, Kontich, Belgium). Scans were performed with the following scanner settings: X-ray source voltage of 70 kVp, current of 140 μA, a 0.5-mm thick aluminum filter to reduce beam-hardening artifacts, and five-frame averaging. The pixel size was 13.5μm, the exposure time was 1780ms, and the rotation step was 0.4°, completing a full rotation over 180°. 2D and 3D images were obtained using Data Viewer (SkyScan) and CTvox (Bruker) to compare anatomical changes in the articular structure.

Even after 6 and 12 weeks, the initial defect structure was identifiable in the direction of the bone trabecular, which can be then designated as the Region of Interest (ROI). To evaluate the area of bone generation instead of bone density, the empty space between the bone trabecular were filled. The area within the ROI was measured, and the area was evaluated by averaging the area of 5 images at 0.135mm intervals. In this methodology, we assessed bone generation, expansion capability, and space maintenance (Figure 6).

A. Bone generation

There were limitations in evaluating scaffold bone generation in the entire ROI area. This is due to the faster bone generation occurring within the defects compared to the scaffolds. This phenomenon is attributed to the comprehensive surrounding of the defects by periosteum and the abundance of osteoblasts in rabbit iliac undercut model, which is unlike the oral and maxillofacial regions. Therefore, we evaluated bone generation within scaffolds specifically in the initial graft material area, to exclude the bone generation of the defect area (Figure 7). Since the scaffold has almost filled with bone at 12 weeks, bone generation on the scaffold was evaluated at 6weeks.

B. Expansion capability

The expanded area of the 4D scaffold appears within the triangular area of the trapezoid.

When applying a non-expanding 3D scaffold, the shaded area within this triangular area represents the defect area where bone was not formed. However, when applying an expanding 4D scaffold, the shaded area within the triangular area represents the combined area of the expanded area and defect area, excluding bone generated area. Therefore, we assessed the expanded area of the 4D scaffold by comparing the shaded areas within the triangular area between 3D,4D scaffolds (Figure 8). Since the expanded area was nearly filled with bone at 12 weeks, the expanded area of the 4D scaffold in triangular area was evaluated at 6weeks.

C. Maintenance of the initial structure

In the craniomaxillofacial area, where facial deformation and function are critical, assessing whether bone generation has aligned with the shape of the existing defect is an important evaluation factor. We measured bone heights H1 and H2 within the designated ROI area and assessed the scaffold's capacity for maintenance of the initial structure by evaluating the extent of bone generation relative to the initial trapezoidal defect (Figure 9).

5. Histological analysis

The tissues were taken after sacrifice and fixed in 10% Neutral Buffered Formalin. Next, the samples were decalcified in Calci-Clear Rapid (National Diagnostics, Atlanta, GA, USA) and embedded in paraffin blocks for histological evaluation. Sections of 5 μm from the paraffin blocks were stained with H&E and Masson's trichrome staining kit (Abcam, Cambridge, UK).

6. Statistical analysis

The measured values of each item were expressed using the mean value and standard deviation to see if there was a significant difference between the groups in the analysis item values. These values were evaluated for significance at the 95% confidence level (α=0.05) by performing an independent sample t test after performing an equal variance test.

Results

Among the 32 cases, 2 cases were untreated, 16 cases presented a normal healing process, and 14 cases showed an abnormal healing process (Figure 10, 11, 12). Among the 14 cases of abnormal healing, 7 were associated with fractures, and 7 were associated with dislocations (Table 1). Out of the 7 cases that were fractured, there were 5 cases in the defect group (Table 2). In the fractured cases, it was observed that the shape of the iliac bone was deformed with fractured line, simultaneously, bone generation did not occur in the defect area (Figure 12). Dislocation was evaluated on the 3D and 4D scaffolds group. Out of the 7 cases that were dislocated, there were 5 cases in the 3D scaffold group (Table 3). It was observed that almost no bone generation was occurred, when the 4D scaffold was dislocated (Figure 13).

In 16 cases of normal healing, the defect area exhibited more significant bone formation compared to regions where the 3D and 4D scaffolds were implanted. These results were attributed to the abundance of osteoblast cells and the rapid bone generation in the rabbit iliac bone. However, through these results, the region where the scaffold is positioned appeared shaded in the CT images, facilitating the identification of both the location and shape of the scaffold. Consequently, the CT analysis enables the assessment of bone formation, expansion capacity, and maintenance of the initial structure.

1. Bone generation

In the rectangular area, which is the initial graft material area, the 4D scaffold group showed an average bone regeneration of 29.16% and the 3D scaffold group showed an average bone generation of 7.82%. The difference between these two groups was statistically significant according to the t-test ($p\ value < 0.001$) (Figure 14).

2. Expansion capability

In the shaded triangular area, representing the defect area for the 3D scaffold group and the combined defect area plus the expanded area minus the bone generation for the 4D scaffold group, the average area occupied was 12.1% for the 4D scaffold group and 2.6% for the 3D scaffold group. The observed difference between these two groups was found to be statistically significant based on the t-test results (*p-value < 0.001*) (Figure 15).

3. Maintenance of the initial structure

To evaluate the maintenance of the initial structure, bone height (H1, H2) was measured. Within the defect group, bone heights H1 and H2 averaged 60.1% and 68.2%, respectively. In the 3D scaffold group, bone heights H1 and H2 averaged 70.1% and 82.8%, respectively. In the 4D scaffold, bone heights H1 and H2 averaged 83.2 and 87.2% respectively. It was confirmed that the 4D scaffold exhibited the most effective space maintenance compared to the other groups (Figure 16). The differences between 4D scaffold group and the other groups were found to be statistically significant according to the t-test (*p value < 0.01*) (Table 4).

4. Histopathological evaluation

Figure 17 represented tissue images obtained through Masson's Trichrome staining. The asterisks indicate the defect area. In the 4D scaffold group, the defect is empty, and in the 3D scaffold group, the defect is filled with muscle. Furthermore, in the 4D scaffold group, active new bone formation is observed along the edges of the defect. But the 3D scaffold group did not exhibit bone formation as actively as observed in the 4D scaffold group.

Figure 18 and 19 represented tissue images obtained through H&E staining. It can be seen that more monocyte and neutrophil due to inflammatory reaction are observed in the 3D scaffold group than in the 4D scaffold group.

Discussion

Out of the total 30 cases, 16 cases (55%) showed a normal healing process. There were two causes of failure: fracture accounted for 7 cases (23%), and graft material dislocation accounted for 7 cases (23%). The causes of fracture and dislocation were due to the strong pelvis muscle force of the rabbit. Muscles surrounding both lateral sides of the undercut area can exert pressure, potentially resulting in fractures and dislocation (Figure 20). Among cases where fractures occurred, 71.4% were defect group. The application of scaffold helped distribute the force exerted on the bone. However, in the defect group, this force distribution does not occur effectively, thereby increasing the probability of fractures. In the cases where dislocation occurred, 71.4% were 3D scaffold group and 28.6% were 4D scaffold group. The low dislocation rate with the 4D scaffold can be attributed to the membrane of the scaffold, providing protection from surrounding muscles and enhancing stability. Moreover, the expansion of the 4D scaffold can restrict displacement from the undercut defect, resulting in lower rate of the dislocation. However, when dislocation occurred with the 4D scaffold, bone generation appeared to rarely occur. Despite the dislocation of the scaffold in the 4D scaffold complex, the membrane of the 4D scaffold complex would still retain the position at the defect. Since the membrane disturbed the infiltration of surrounding tissues, it might limit the process of bone generation (Figure 13b and c).

In the bone generation analysis, the 4D scaffold group showed an average bone generation of 29.16% and the 3D scaffold group showed an average bone generation of 7.82%. The 3D scaffold is composed of PCL, known for its hydrophobic nature, posing challenges for stable cell adhesion. Consequently, it is evident that osteoblasts faced difficulty in adhering to the scaffold, consequently leading to a slower bone generation process. On the contrary, the 4D scaffold overcame these limitations by utilizing a hyaluronic acid, promoting better cell retention and growth, resulting in enhanced bone generation. In the expansion capability analysis, it was observed that the shaded area of the 4D scaffold group was larger than that of the 3D scaffold group. In the 4D scaffold group, the

shaded area represents the defect area plus the expanded area minus the bone generation, whereas in the 3D scaffold group, it signifies solely the defect area. The larger shaded area in the 4D scaffold serves as evidence of its in vivo expansion capability, demonstrating how the scaffold expanded within the biological environment. In the analysis of space maintenance, at 12 weeks, the 4D scaffold demonstrated better maintenance of initial structure compared to the other groups. The 4D scaffold maintained a bone height between 83% and 87% of the initial bone height. This demonstrates that, after the bone defect healing process, the 4D scaffold group can nearly reconstruct to its original structure. The remarkable preservation of the original structure within the 4D group can be attributed to its expansion capability and superior bone generation. Particularly in regions affecting facial aesthetics, like the craniomaxillofacial area, preserving the original shape of the bone defect during healing and reconstruction is crucial in bone grafting.

According to histopathological analysis, the 4D scaffold showed more active new bone formation compared to the 3D scaffold, and exhibited less inflammatory response. it can be confirmed that the 4D scaffold is a more biocompatible material compared to the 3D scaffold and induces bone generation more effectively. Additionally, within the defect area, it was observed that the 3D scaffold was filled with muscle tissue, whereas the 4D scaffold remained as an empty space. This observation suggests that the membrane present in the 4D scaffold contributed to space maintenance. In many clinical applications when using the 3D scaffold, the 3D scaffold can be applied without requiring a membrane[25]. This is because there is a dead space that the 3D scaffold cannot fill within the defect area, and when a membrane prevents infiltration of surrounding tissues, blood and exudate might be accumulated, promoting to bacterial proliferation and subsequently triggering inflammatory reactions. However, if the procedure is carried out without a membrane, as in this experiment, infiltration of surrounding tissues into the defect area occurs. This makes it difficult for bone generation to proceed in the original structure pattern, as tissues invade the space intended for bone growth. However, the 4D scaffold reduces dead space due to expansion and exhibits space stability and maintenance, confirming its capability for bone generation.

There were limitations in this experiment. We created a trapezoid bone defect at the rabbit iliac crest due to insufficient bone size and thickness on the cranial bone. But it has different conditions compared to the clinical craniomaxillofacial region. The iliac bone has abundant osteoblast cells compared to cranial bone. These abundant osteoblast cells and the rapid growth in rabbits facilitated even more effective bone generation. Moreover, in this experiment, as the defects were intentionally induced, the periosteum naturally covered the top and lateral sides of the defects. As a result, adequate blood circulation and nutrient were supplied, and osteoblasts were easily attached. These conditions also facilitated efficient bone generation. At the defect site, these conditions supported faster bone formation outside the scaffold rather than inside it, as the scaffolds only functioned for osteoconduction rather than osteoinduction and osteogenesis. Hence, we couldn't compare the bone generation in the defect group with that of the scaffold groups (3D, 4D). However, scaffolds serve as valuable materials for bone regeneration in the craniomaxillofacial area [26]. In the craniomaxillofacial region, cranial bones have fewer osteoblasts compared to the iliac bone, and the bone defect area is often covered by only a small portion of periosteum. As result, bone healing is slow. Therefore, scaffolds serve as valuable materials for bone reconstruction, providing osteoconduction and preventing the infiltration of other tissue cells.

Despite these adverse conditions, in this experiment, the 4D scaffold demonstrated the expansion capability in vivo environments and superior bone generation and preservation of original structures than 3D conventional scaffolds. This novel 4D scaffold could be a promising substitute for conventional bone graft system in the maxillofacial area, and it could further extend its application to the fields of the orthopedic and plastic surgery. Based on these study results, additional long term large animal study and clinical study are needed.

Conclusion

This study emphasizes the significance of scaffold development for craniomaxillofacial area reconstruction. It introduces 4D printing technology utilizing conventional materials, particularly the hyaluronic acid-based and PCL scaffold. We termed it a 4D scaffold because of its capability to expand over time, according to the shape of the defect. Despite the differences from the conditions in the craniomaxillofacial area and the rabbit iliac crest model employed in this study, we were able to confirm the 4D scaffold's bone generation, expansion capability, and maintenance of the initial structure. Furthermore, on histological examination, it was found that the 4D scaffold exhibited better bone generation and less inflammatory response compared to the 3D scaffold. Although further research involving large and long-term animal trials and clinical investigations is necessary to validate the practicality of the 4D scaffold in real clinical models, this study emphasizes the potential of 4D printing in scaffold design. It offers a customized solution for complex bone defects in various clinical applications

References

1. Kim SS, Sun Park M, Jeon O, Yong Choi C, Kim BS. Poly(lactide-co-glycolide)/hydroxyapatite composite scaffolds for bone tissue engineering. Biomaterials. 2006;27(8):1399-409.
2. Jeon BJ, Jeong SY, Koo AN, Kim B-C, Hwang Y-S, Lee SC. Fabrication of porous PLGA microspheres with BMP-2 releasing polyphosphate-functionalized nano-hydroxyapatite for enhanced bone regeneration. Macromolecular Research. 2012;20(7):715-24.
3. Son JS, Kim SG, Oh JS, Appleford M, Oh S, Ong JL, et al. Hydroxyapatite/polylactide

biphasic combination scaffold loaded with dexamethasone for bone regeneration. J Biomed Mater Res A. 2011;99(4):638-47.

4. Cho YS, Hong MW, Quan M, Kim SY, Lee SH, Lee SJ, et al. Assessments for bone regeneration using the polycaprolactone SLUP (salt-leaching using powder) scaffold. J Biomed Mater Res A. 2017;105(12):3432-44.
5. Cho YS, Kim B-S, You H-K, Cho Y-S. A novel technique for scaffold fabrication: SLUP (salt leaching using powder). Current Applied Physics. 2014;14(3):371-7.
6. Sadiasa A, Nguyen TH, Lee BT. In vitro and in vivo evaluation of porous PCL-PLLA 3D polymer scaffolds fabricated via salt leaching method for bone tissue engineering applications. J Biomater Sci Polym Ed. 2014;25(2):150-67.
7. Shahabipour F, Ashammakhi N, Oskuee RK, Bonakdar S, Hoffman T, Shokrgozar MA, et al. Key components of engineering vascularized 3-dimensional bioprinted bone constructs. Transl Res. 2020;216:57-76.
8. Zhang S, Dong Y, Chen M, Xu Y, Ping J, Chen W, et al. Recent developments in strontium-based biocomposites for bone regeneration. J Artif Organs. 2020;23(3):191-202.
9. Lai WY, Chen YJ, Lee AK, Lin YH, Liu YW, Shie MY. Therapeutic effects of the addition of fibroblast growth factor-2 to biodegradable gelatin/magnesium-doped calcium silicate hybrid 3D-printed scaffold with enhanced osteogenic capabilities for critical bone defect restoration. Biomedicines. 2021;9(7):712.
10. Lee KG, Lee KS, Kang YJ, Hwang JH, Lee SH, Park SH, et al. Rabbit calvarial defect model for customized 3D-printed bone grafts. Tissue Eng Part C Methods. 2018;24(5):255-62.
11. Ghim M-S, Choi E-Y, Kim YY, Cho Y-S. Quantitative analysis of bone regeneration efficacy as shape conformity of scaffold: Evidence for importance of additive-manufacturing precision in tissue engineering. Materials & Design. 2023;231:112073.
12. Lee SH, Lee KG, Hwang JH, Cho YS, Lee KS, Jeong HJ, et al. Evaluation of mechanical strength and bone regeneration ability of 3D printed kagome-structure scaffold using rabbit

calvarial defect model. Mater Sci Eng C Mater Biol Appl. 2019;98:949-59.

13. Xie R, Hu J, Hoffmann O, Zhang Y, Ng F, Qin T, et al. Self-fitting shape memory polymer foam inducing bone regeneration: a rabbit femoral defect study. Biochim Biophys Acta Gen Subj. 2018;1862(4):936-45.

14. Wang C, Yue H, Liu J, Zhao Q, He Z, Li K, et al. Advanced reconfigurable scaffolds fabricated by 4D printing for treating critical-size bone defects of irregular shapes. Biofabrication. 2020;12(4):045025.

15. Zhang F, Wen N, Wang L, Bai Y, Leng J. Design of 4D printed shape-changing tracheal stent and remote controlling actuation. International Journal of Smart and Nano Materials. 2021;12(4):375-89.

16. Xue Y, Chen H, Xu C, Yu D, Xu H, Hu Y. Synthesis of hyaluronic acid hydrogels by crosslinking the mixture of high-molecular-weight hyaluronic acid and low-molecular-weight hyaluronic acid with 1,4-butanediol diglycidyl ether. RSC Adv. 2020;10(12):7206-13.

17. Xue L, Deng T, Guo R, Peng L, Guo J, Tang F, et al. A composite hydrogel containing mesoporous silica nanoparticles loaded with artemisia argyi extract for improving chronic wound healing. Front Bioeng Biotechnol. 2022;10:825339.

18. Park S, Park KY, Yeo IK, Cho SY, Ah YC, Koh HJ, et al. Investigation of the degradation-retarding effect caused by the low swelling capacity of a novel hyaluronic acid filler developed by solid-phase crosslinking technology. Ann Dermatol. 2014;26(3):357-62.

19. Park TH, Seo SW, Kim JK, Chang CH. Clinical experience with hyaluronic acid-filler complications. J Plast Reconstr Aesthet Surg. 2011;64(7):892-6.

20. Fakhari A, Berkland C. Applications and emerging trends of hyaluronic acid in tissue engineering, as a dermal filler and in osteoarthritis treatment. Acta Biomater. 2013;9(7):7081-92.

21. Mei P, Wu R, Shi S, Li B, Ma C, Hu B, et al. Conjugating hyaluronic acid with porous biomass to construct anti-adhesive sponges for rapid uranium extraction from seawater.

Chemical Engineering Journal. 2021;420:130382.

22. Dinh L, Hong J, Min Kim D, Lee G, Jung Park E, Hyuk Baik S, et al. A novel thermosensitive poloxamer-hyaluronic acid- kappa-carrageenan-based hydrogel anti-adhesive agent loaded with 5-fluorouracil: a preclinical study in Sprague-Dawley rats. Int J Pharm. 2022;621:121771.

23. Bukhari SNA, Roswandi NL, Waqas M, Habib H, Hussain F, Khan S, et al. Hyaluronic acid, a promising skin rejuvenating biomedicine: a review of recent updates and pre-clinical and clinical investigations on cosmetic and nutricosmetic effects. Int J Biol Macromol. 2018;120(Pt B):1682-95.

24. Al-Halaseh LK, Al-Jawabri NA, Tarawneh SK, Al-Qdah WK, Abu-Hajleh MN, Al-Samydai AM, et al. A review of the cosmetic use and potentially therapeutic importance of hyaluronic acid. Journal of Applied Pharmaceutical Science. 2022;12(7):034-41.

25. Lopez CD, Diaz-Siso JR, Witek L, Bekisz JM, Cronstein BN, Torroni A, et al. Three dimensionally printed bioactive ceramic scaffold osseoconduction across critical-sized mandibular defects. journal of surgical research. 2018;223:115-22.

26. Nayak VV, Slavin B, Bergamo ET, Boczar D, Slavin BR, Runyan CM, et al. Bone Tissue Engineering (BTE) of the Craniofacial Skeleton, Part I: Evolution and Optimization of 3D-Printed Scaffolds for Repair of Defects. Journal of Craniofacial Surgery. 2023;34(7):2016-25.

List of tables

Table 1. Distribution of complication cases

	N=7
Defect	5 (71.4%)
3D scaffold	0 (0%)
4D scaffold	2 (28.6%)

Table 2. Distribution of fractured cases

	N=30
Normal healing	16 (53.3%)
Fracture	7 (23.3%)
Dislocation	7 (23.3%)

Table 3. Distribution of dislocated cases

	N=7
3D scaffold	5 (71.4%)
4D scaffold	2 (28.6%)

Table 4. T-test in the maintenance of the initial structure analysis

	Defect&4D	Defect&3D	3D&4D
H1	p <0.001	0.74	p <0.001
H2	p <0.01	0.79	p <0.01

p<0.05 was considered statistically significant

Defect: defect group, 3D: 3D scaffold group, 4D: 4D scaffold group

List of figures

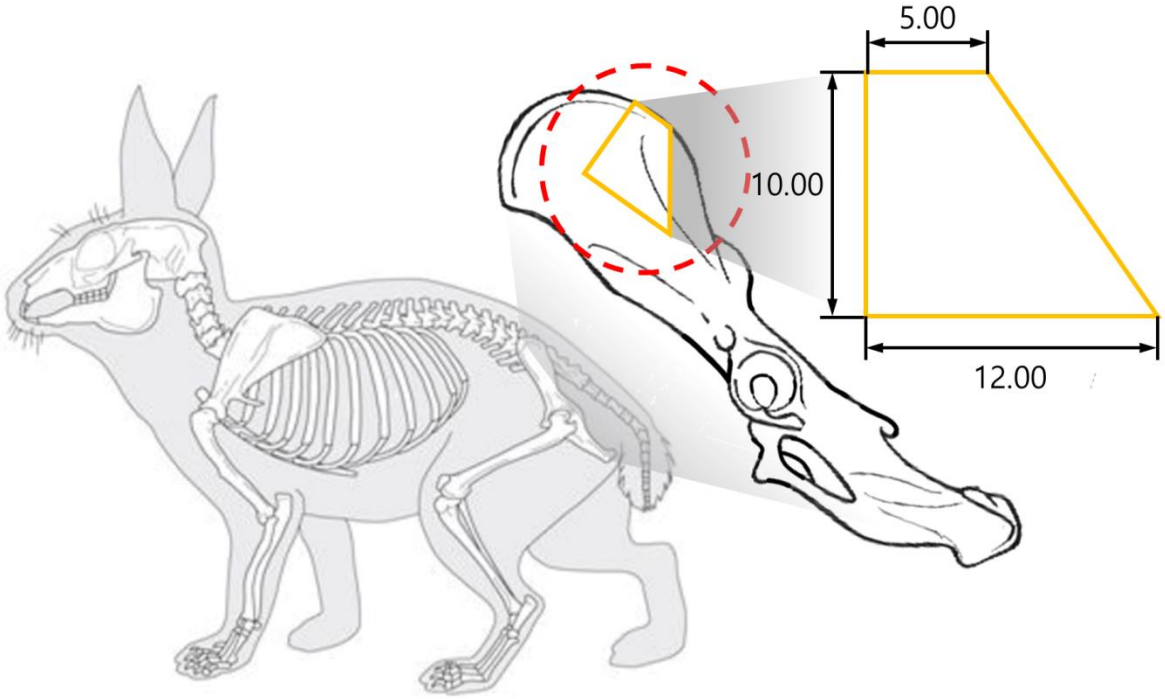

Figure 1. Schematic images of the formation of a trapezoidal defect on the rabbit iliac crest: (top side: 5mm, height: 10mm, bottom side: 12mm).

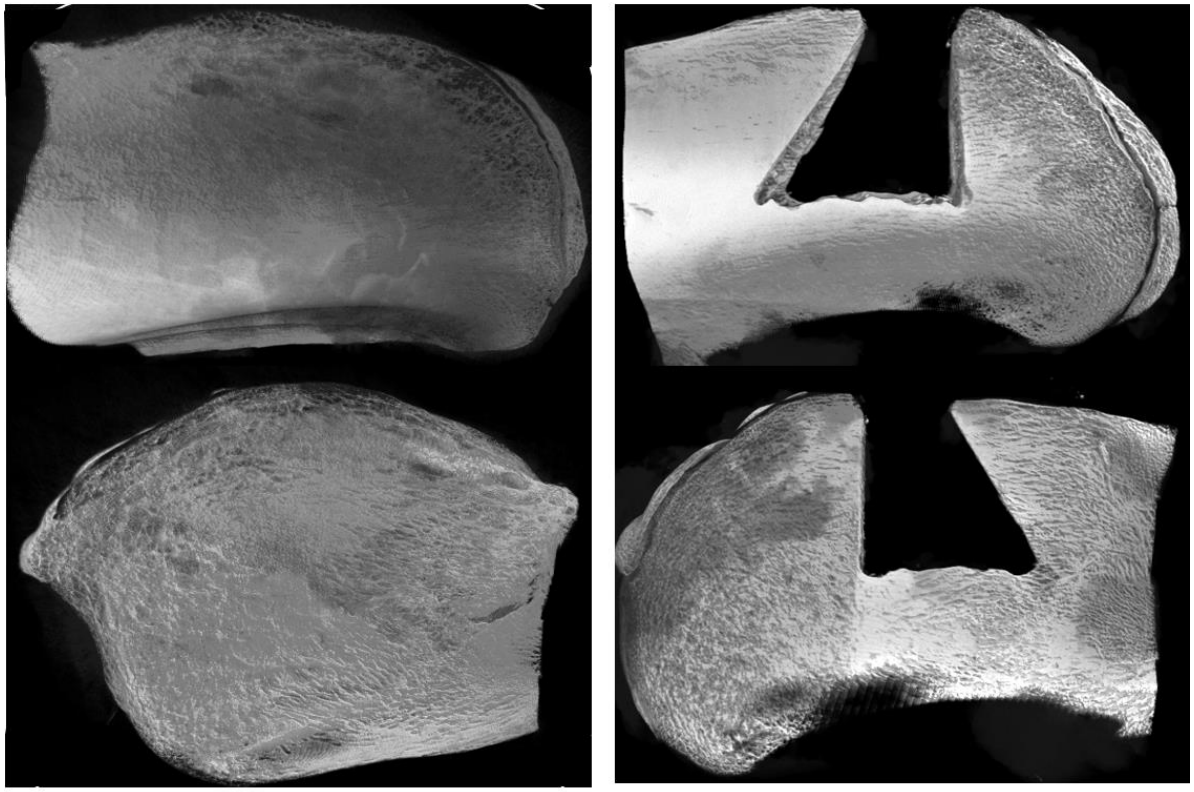

Figure 2. The images taken via ex vivo micro-CT before and after the formation of a trapezoidal defect on the rabbit iliac crest

a) Frontal and posterior images before the surgical procedure. b) Frontal and posterior images after the surgery

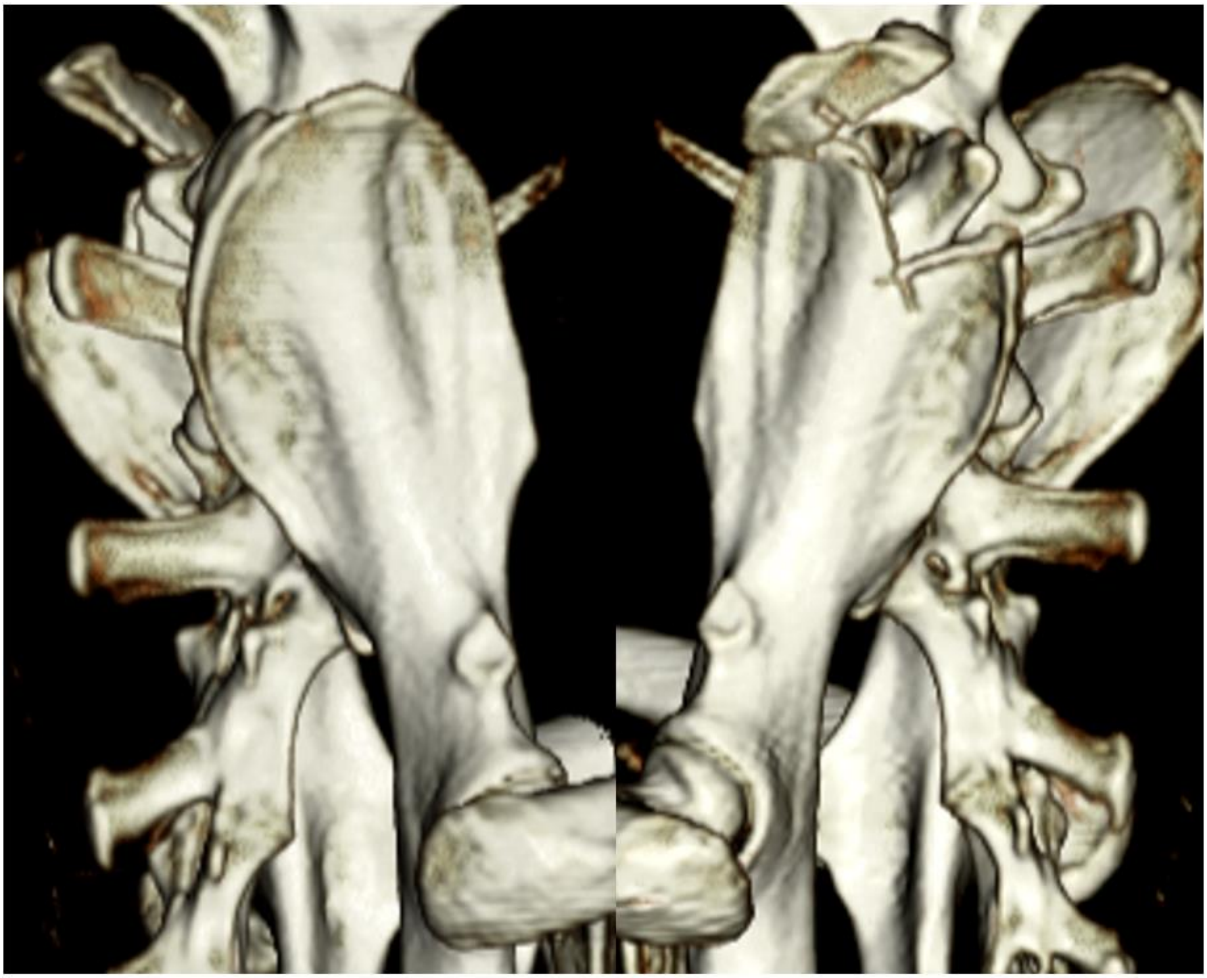

Figure 3. The images taken via Live CT before and after the formation of a trapezoidal defect on the rabbit iliac crest.

a) The image shows the normal iliac crest b) The image shows the formation of Trapezoidal defect

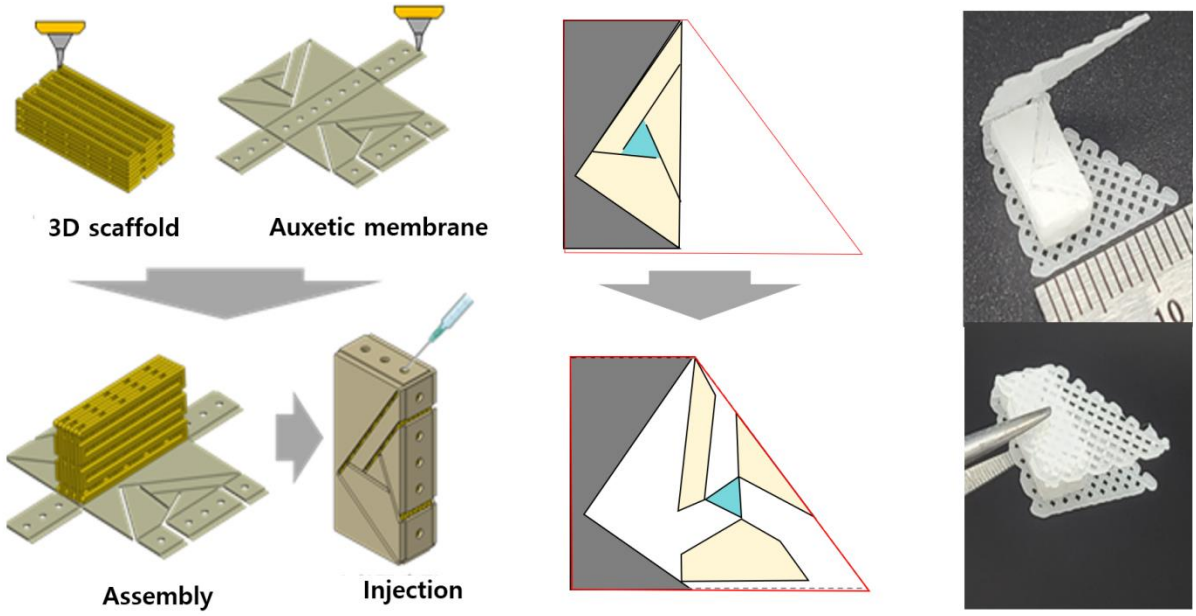

Figure 4. The Manufacturing Process of a 4D scaffold

a) The 4D scaffold is manufactured based on the 3D scaffold, which is surrounded by an auxetic membrane. b) Upon injection, the hyaluronic acid undergoes swelling, effectively retaining surrounding moisture. This process induces the expansion of the auxetic membrane.

c) The completely manufactured 4D scaffold. The membrane was designed to guide the expansion of the 4D scaffold.

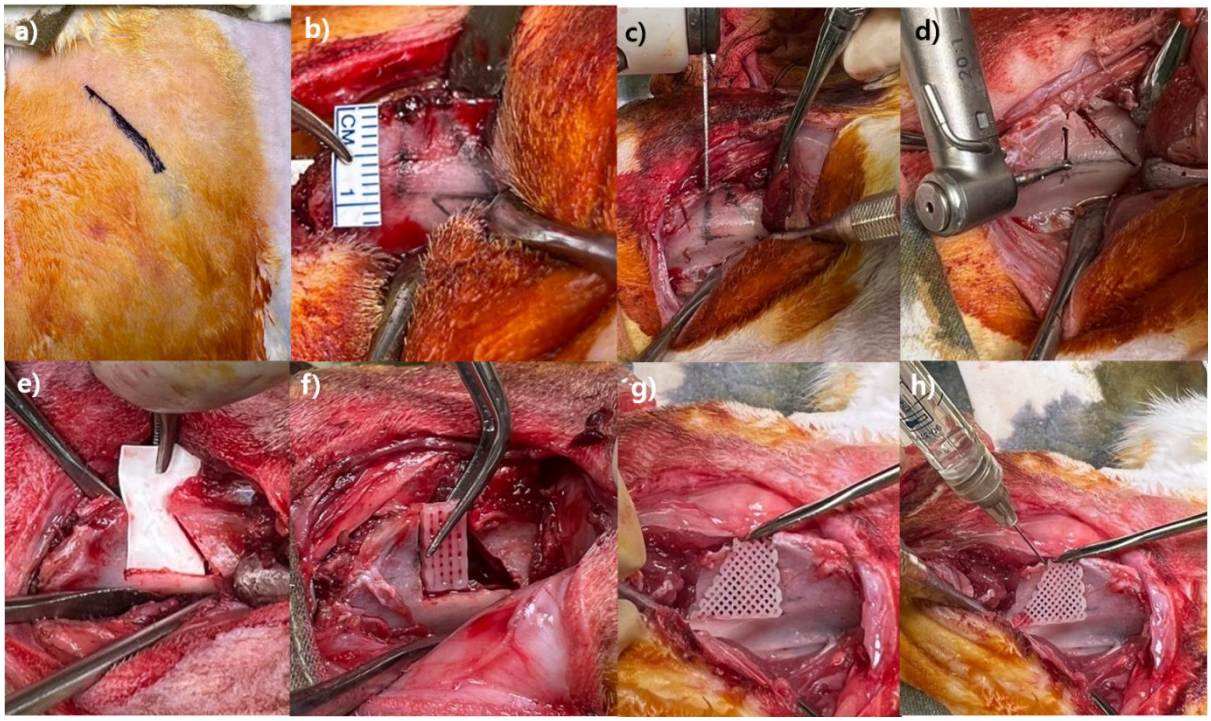

Figure 5. Scaffold implantation into a rabbit iliac bone undercut defect

a) Hair was removed from the rabbit surgical site, followed by disinfection with povidone. The iliac crests on both sides were then marked on the skin using a marking pen. b) Using a ruler, we designed the trapezoidal osteotomy line. c, d, and e) A trapezoidal defect was created using a saw and drill. f) The 3D scaffold was applied to the defect. g and h) The 4D scaffolds were applied, accompanied by the application of the hyaluronic acid to the defect area.

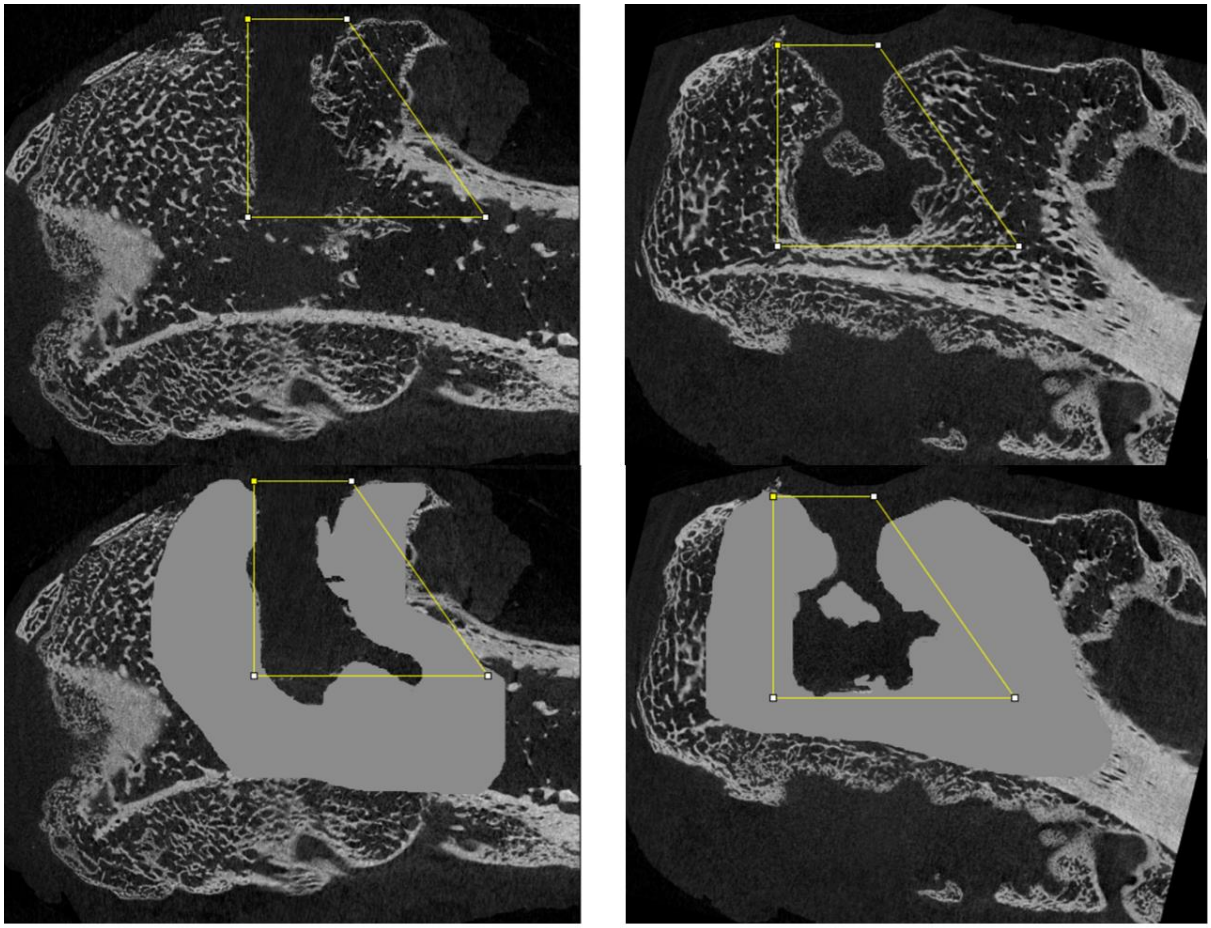

Figure 6. The Region of Interest (ROI) was designated: a) 3D scaffold group, b) 4D scaffold group

The ROI was defined to assess bone regeneration area by filling the gaps between bone trabecular to evaluate the bone generation and expansion capability.

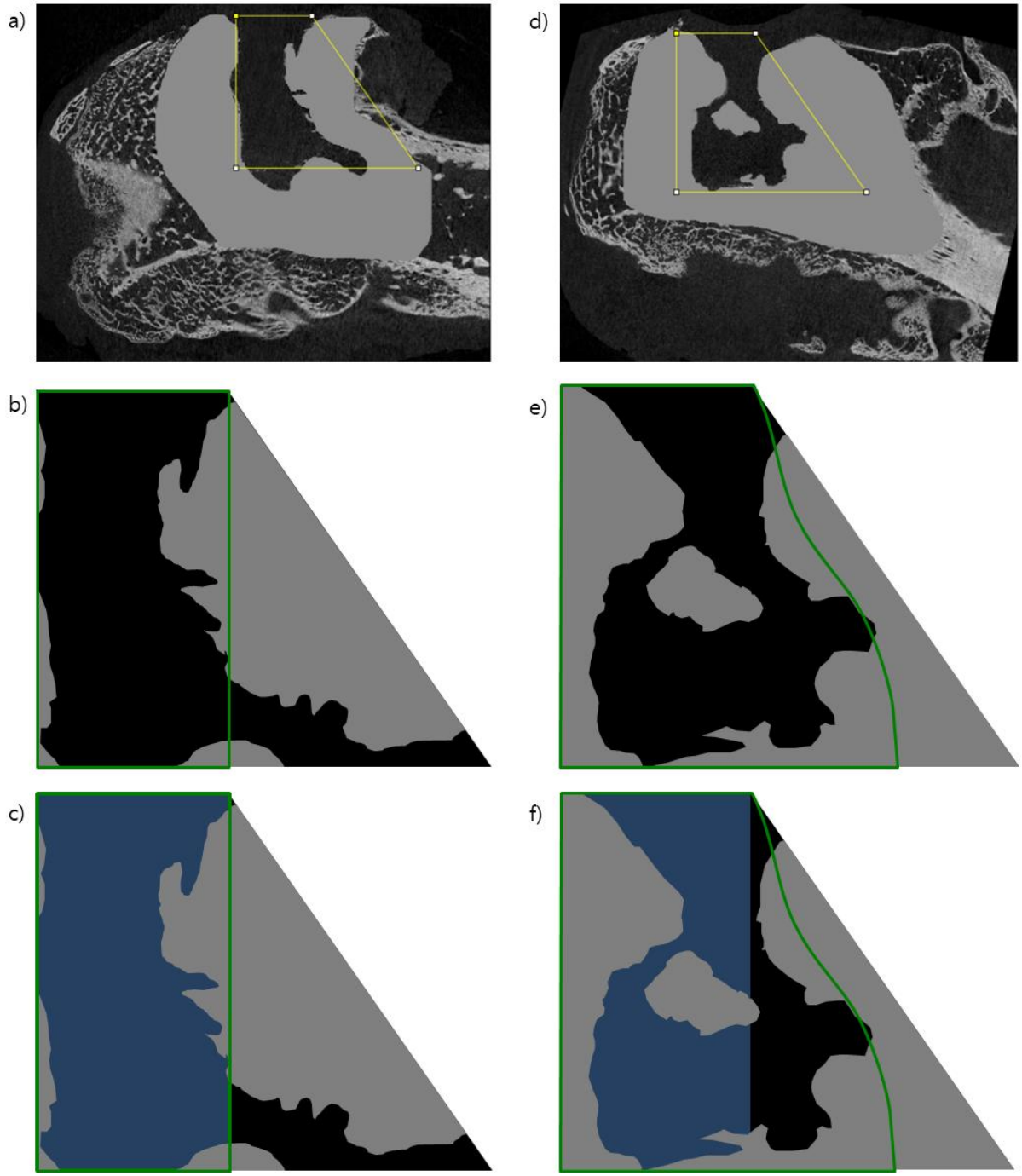

Figure 7. The Region of Interest (ROI) was designated: a) 3D scaffold group, d) 4D scaffold group. Schematic images were designed for the bone generation analysis: b, c) 3D scaffold group & e, f) 4D scaffold group

The scaffold shape is represented by the green line. The expanded 4D scaffold is depicted as having a wider area outlined by the green line. The blue area represents the initial scaffold area where the bone generation analysis was specifically conducted.

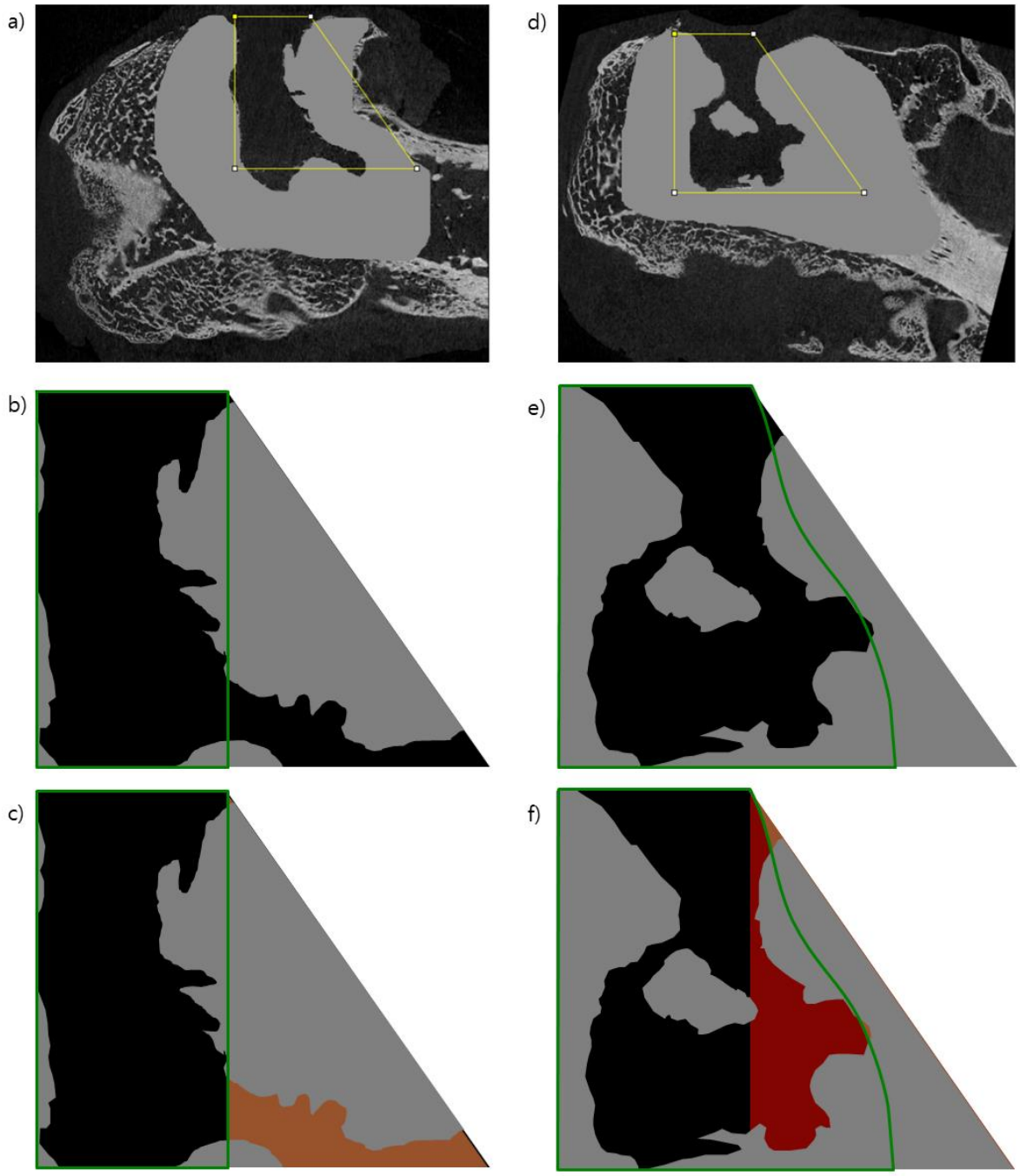

Figure 8. The Region of Interest (ROI) was designated: a) 3D scaffold group, d) 4D scaffold group. Schematic images were designed for the expansion capability analysis: b, c) 3D scaffold group & e, f) 4D scaffold group

The scaffold shape is represented by the green line. The expanded 4D scaffold is depicted as having a wider area outlined by the green line. The red area represents the expanded area, and the orange area represents the defect area. The shaded area in the triangle represents the defect area plus the expanded area minus the bone generation, whereas in the 3D scaffold group, it signifies solely the defect area.

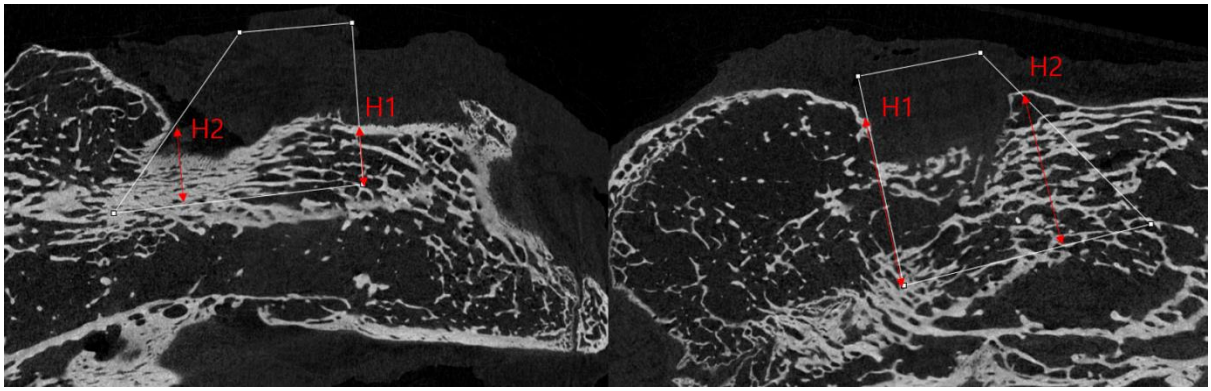

Figure 9. Bone height was measured to evaluate the maintenance of the initial structure during healing process.

Bone heights H1 and H2 was measured within the designated region of interest (ROI) area

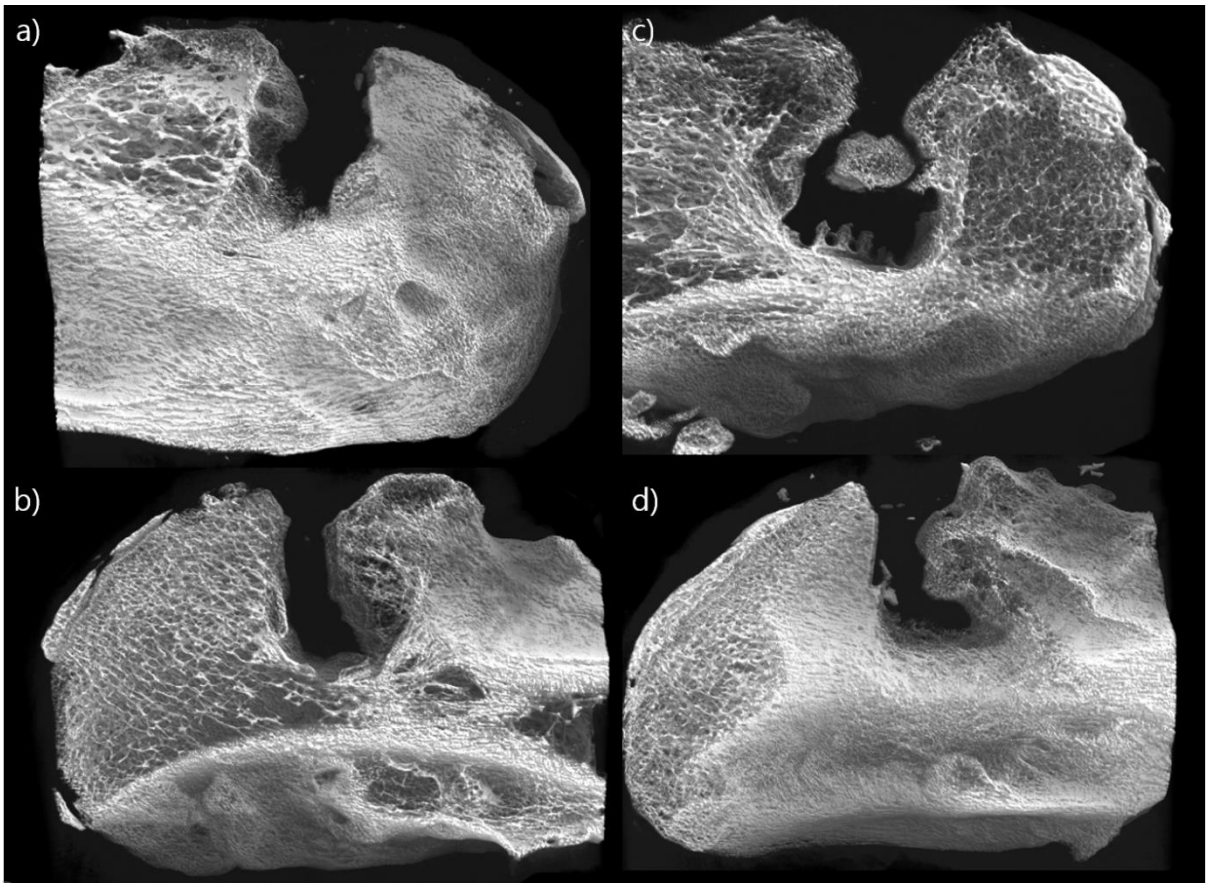

Figure 10. Normal healing cases in CT images at 6weeks: a and b) 3D scaffold group, c and d) 4D scaffold group.

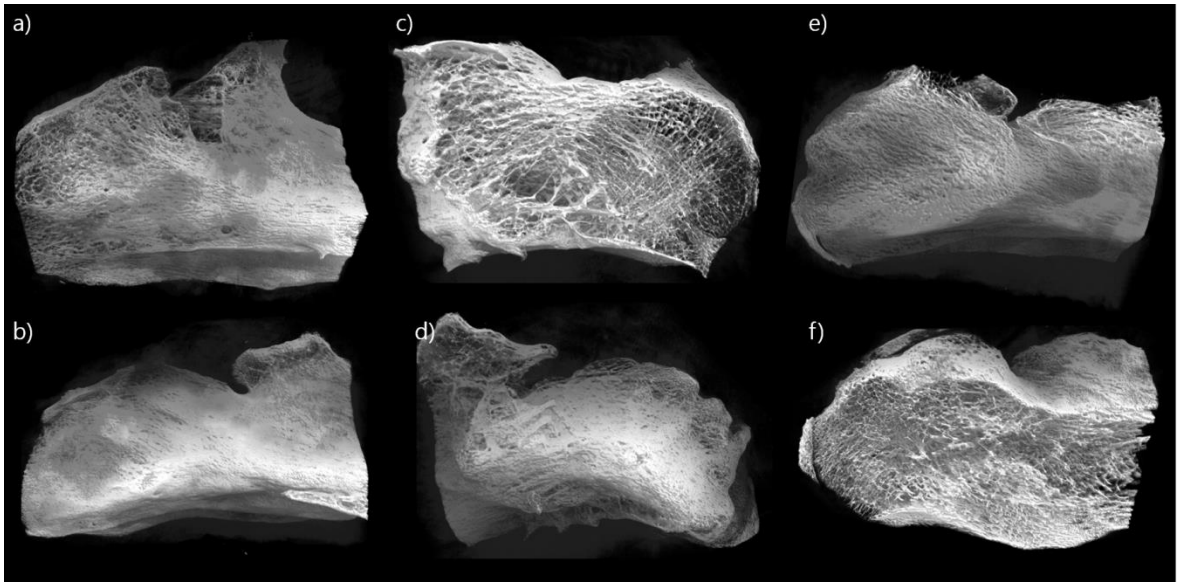

Figure 11. Normal healing cases in CT images at 12 weeks: a and b) 3D scaffold group. c and d) 4D scaffold group. e and f) defect group.

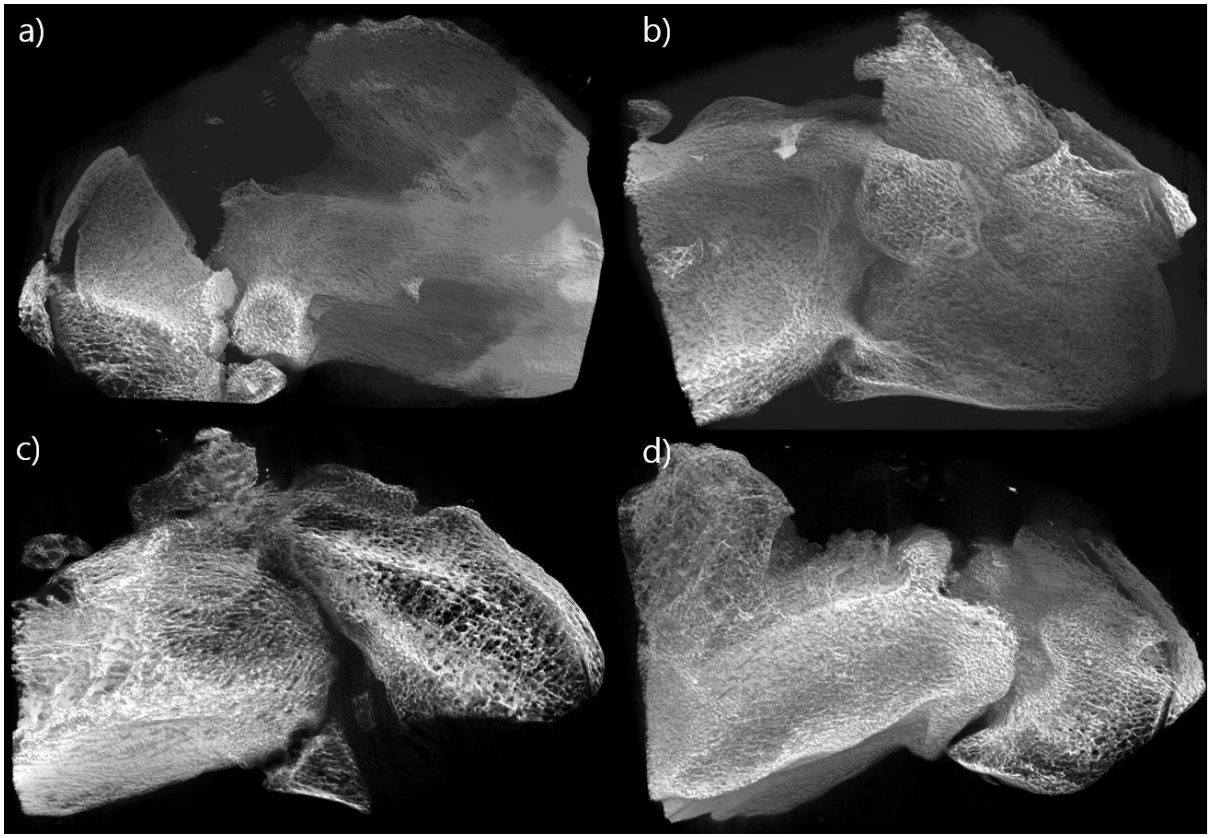

Figure 12. Fractured cases in CT images: a and b) defect group c) 3D scaffold group d) 4D scaffold group.

It was observed that the shape of the iliac bone was deformed with fractured line, simultaneously, bone regeneration did not occur in the defect area.

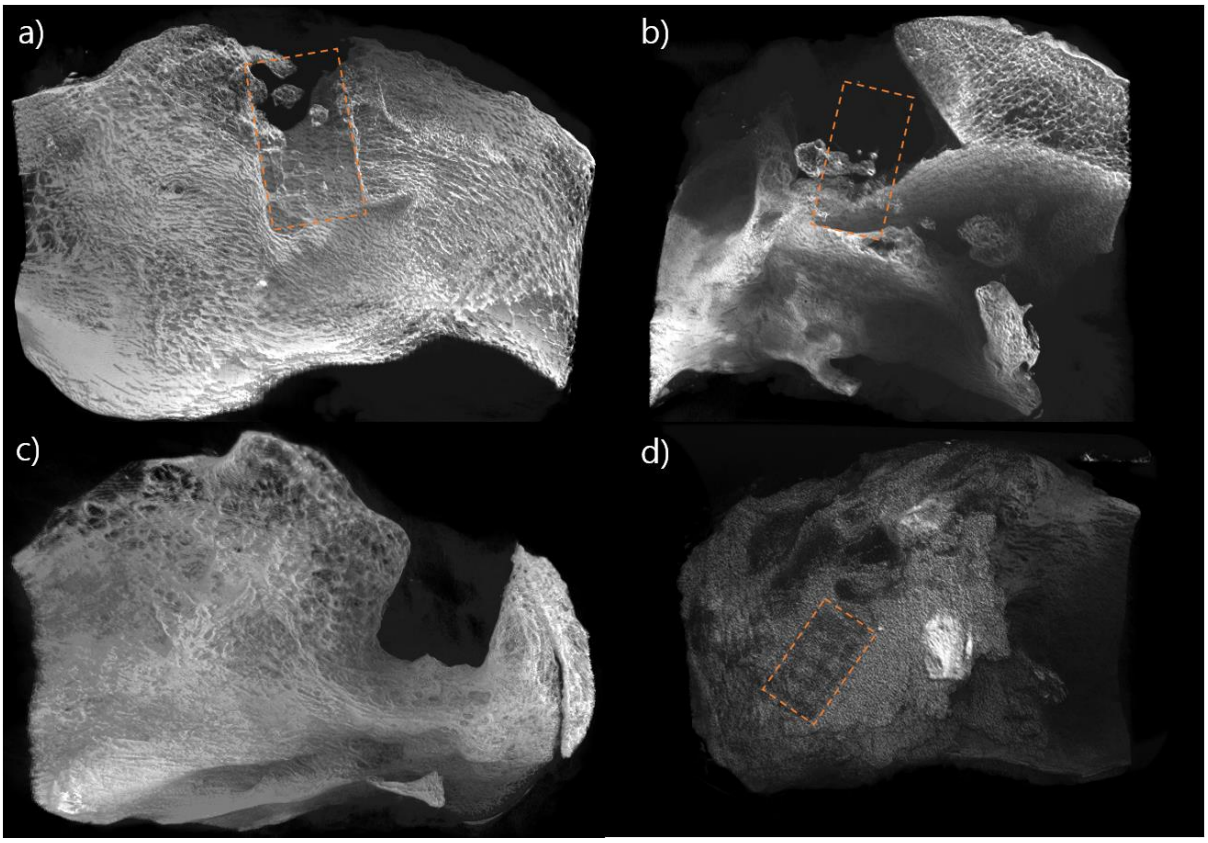

Figure 13. Dislocated cases in CT images: a) 3D scaffold group b) 4D scaffold group c and d) 4D scaffold group in same model.

The images c) and d) are the same model. The scaffolds could be founded in the muscle. Bone generation was observed to be infrequent, when the 4D scaffold underwent dislocation in images b) and c).

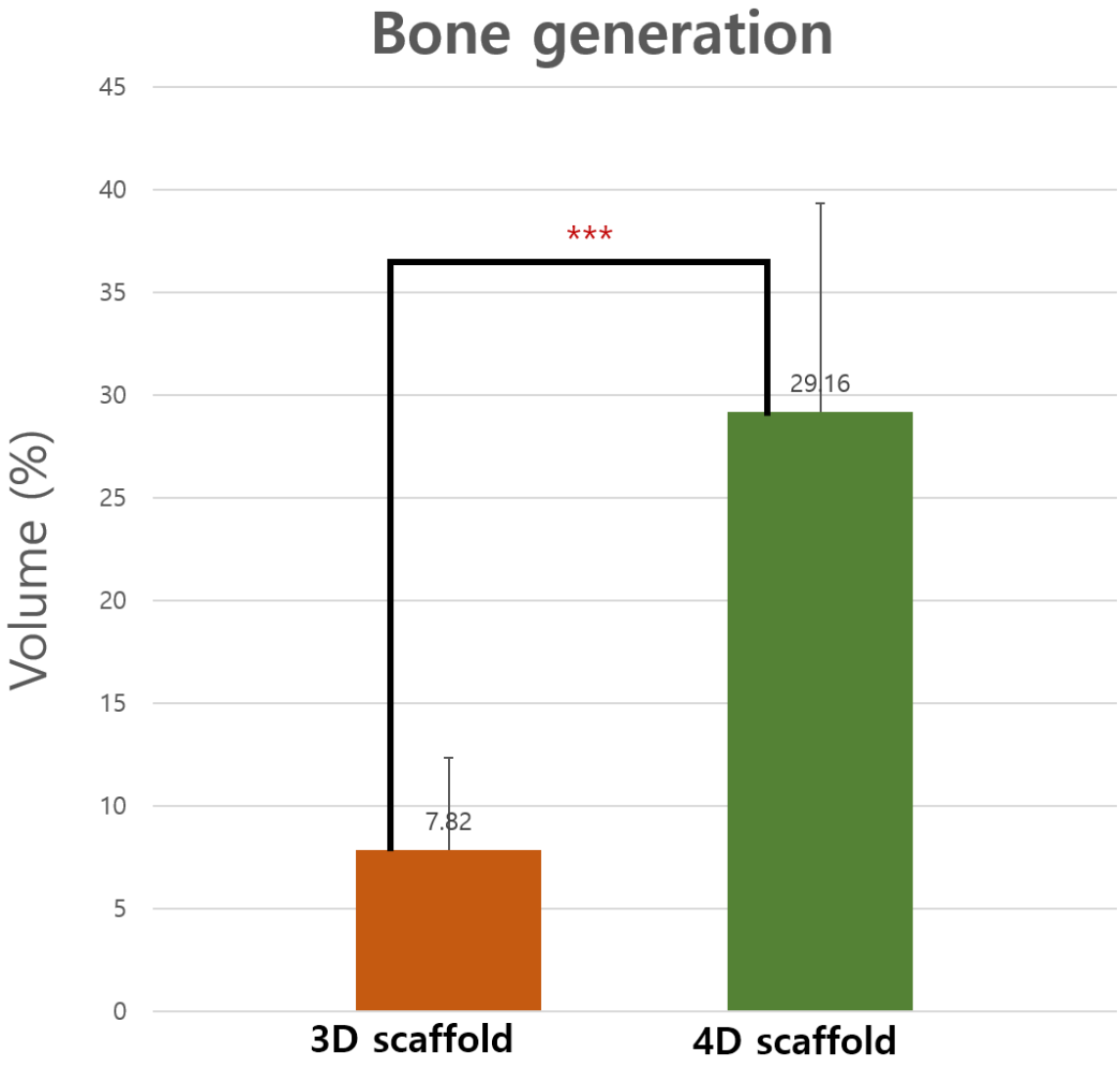

Figure 14. Bone generation analysis of the 3D scaffold group and 4D scaffold group at 6weeks. The statistical significance for bone generation between 3D scaffold and 4D scaffold is indicated by asterisk(s) based on t-test (* p<0.05, ** p<0.01, *** p< 0.001).

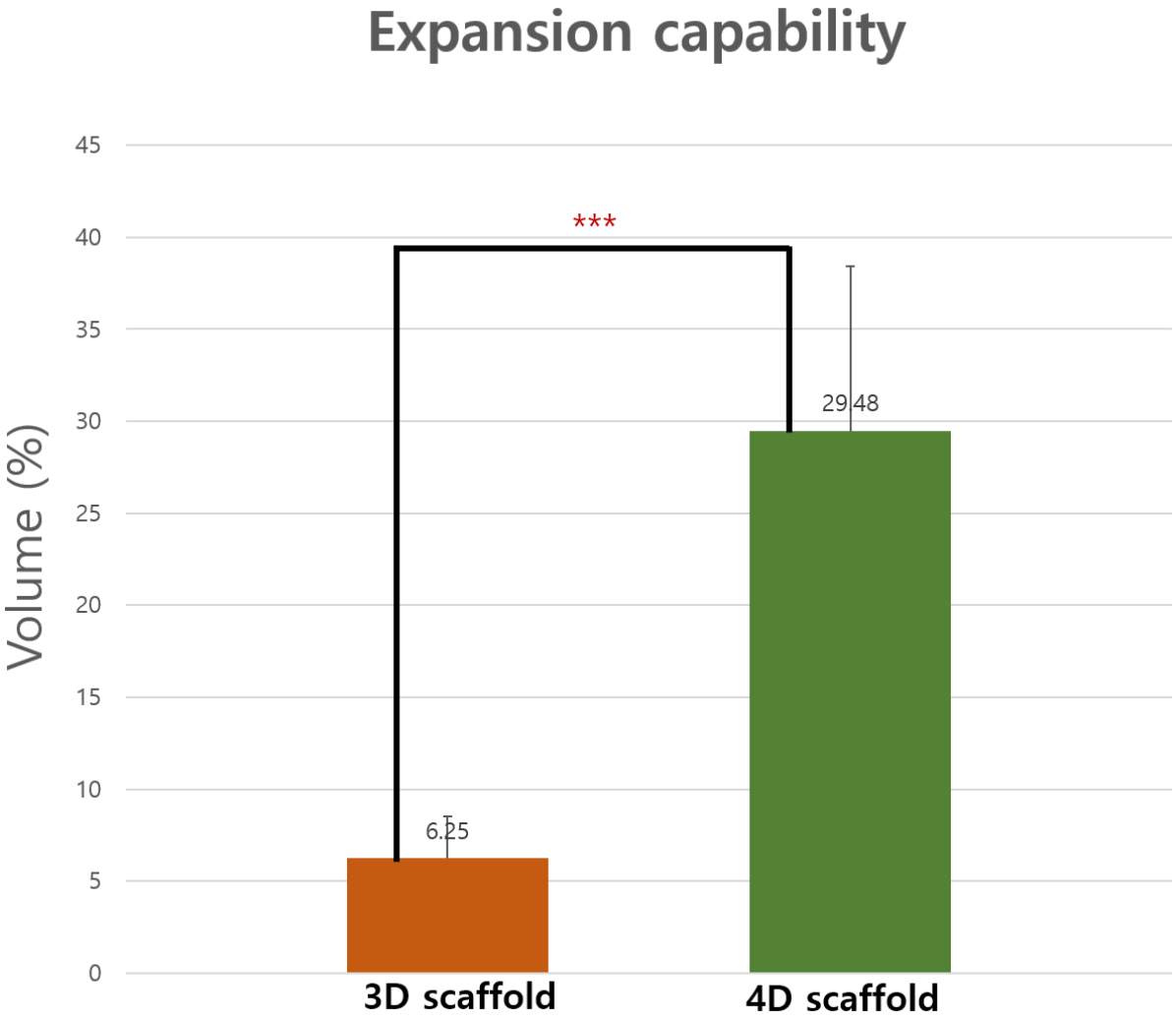

Figure 15. Expansion capability analysis of the 3D scaffold group and 4D scaffold group at 6weeks.

The statistical significance for expansion capability between 3D scaffold and 4D scaffold is indicated by asterisk(s) based on t-test (* p<0.05, ** p<0.01, *** p< 0.001).

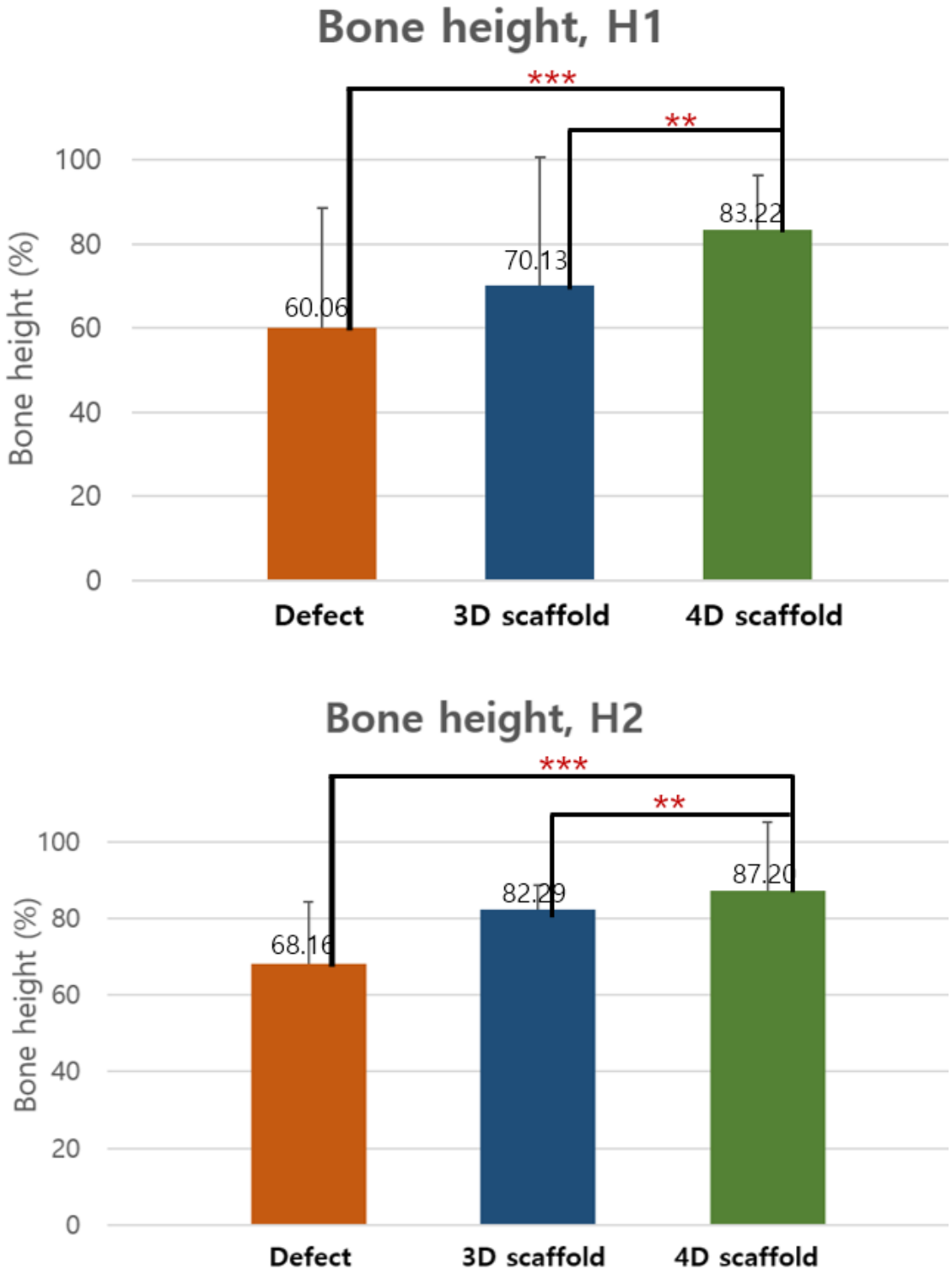

Figure 16. Maintenance of the initial structure analysis of the Defect, the 3D scaffold group, and 4D scaffold group at 12weeks.

The statistical significance for bone heights (H1, H2) between defect group, 3D scaffold group, and 4D scaffold group are indicated by asterisk(s) based on t-test (* p<0.05, ** p<0.01, *** p< 0.001).

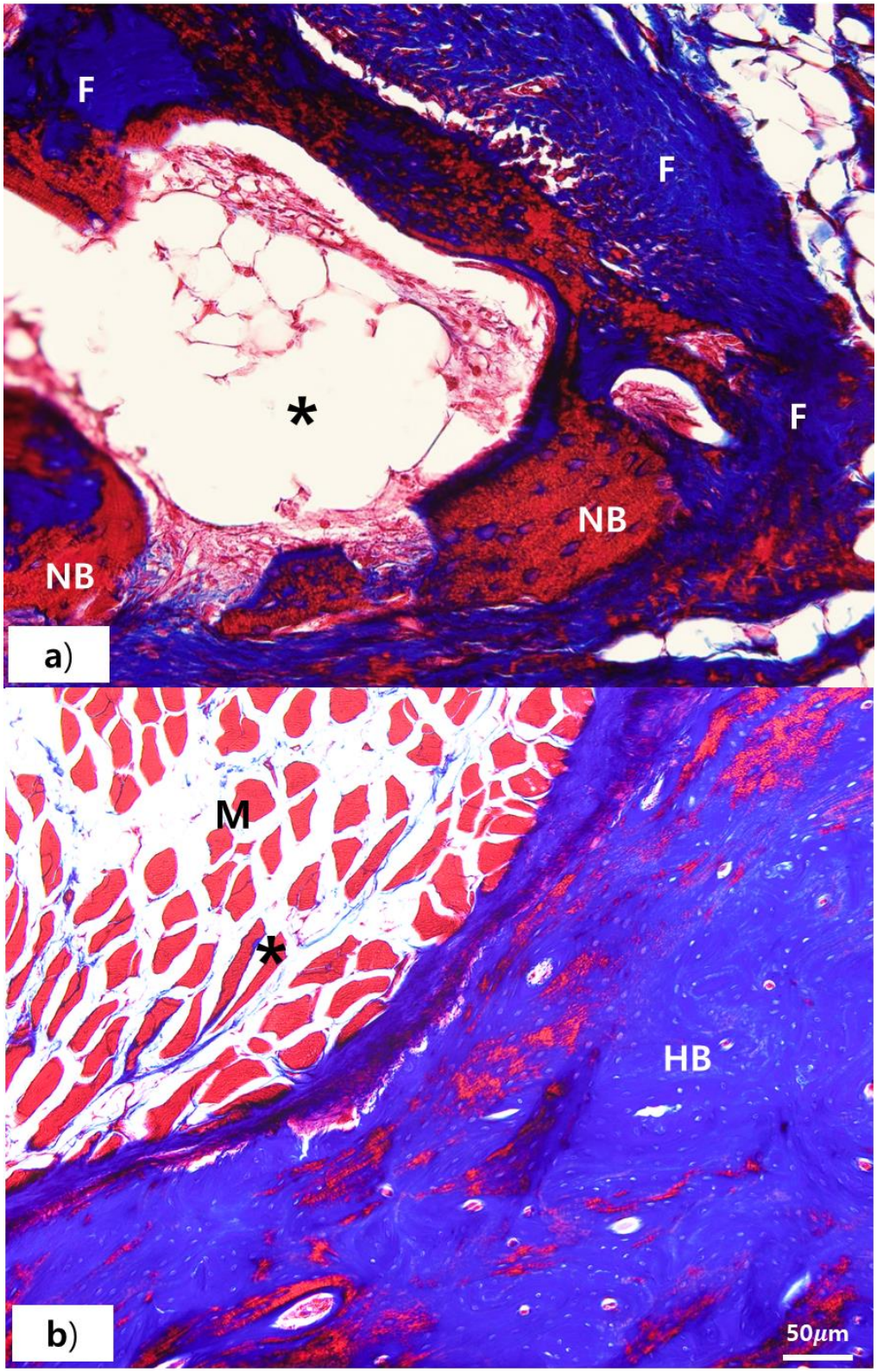

Figure 17. Histological features obtained through Masson's Trichrome staining a) 4D scaffold group b) 3D scaffold group.

Asterisk: defect area, NB: new bone, F: fibrous connective tissue, HB: host bone, M: muscle

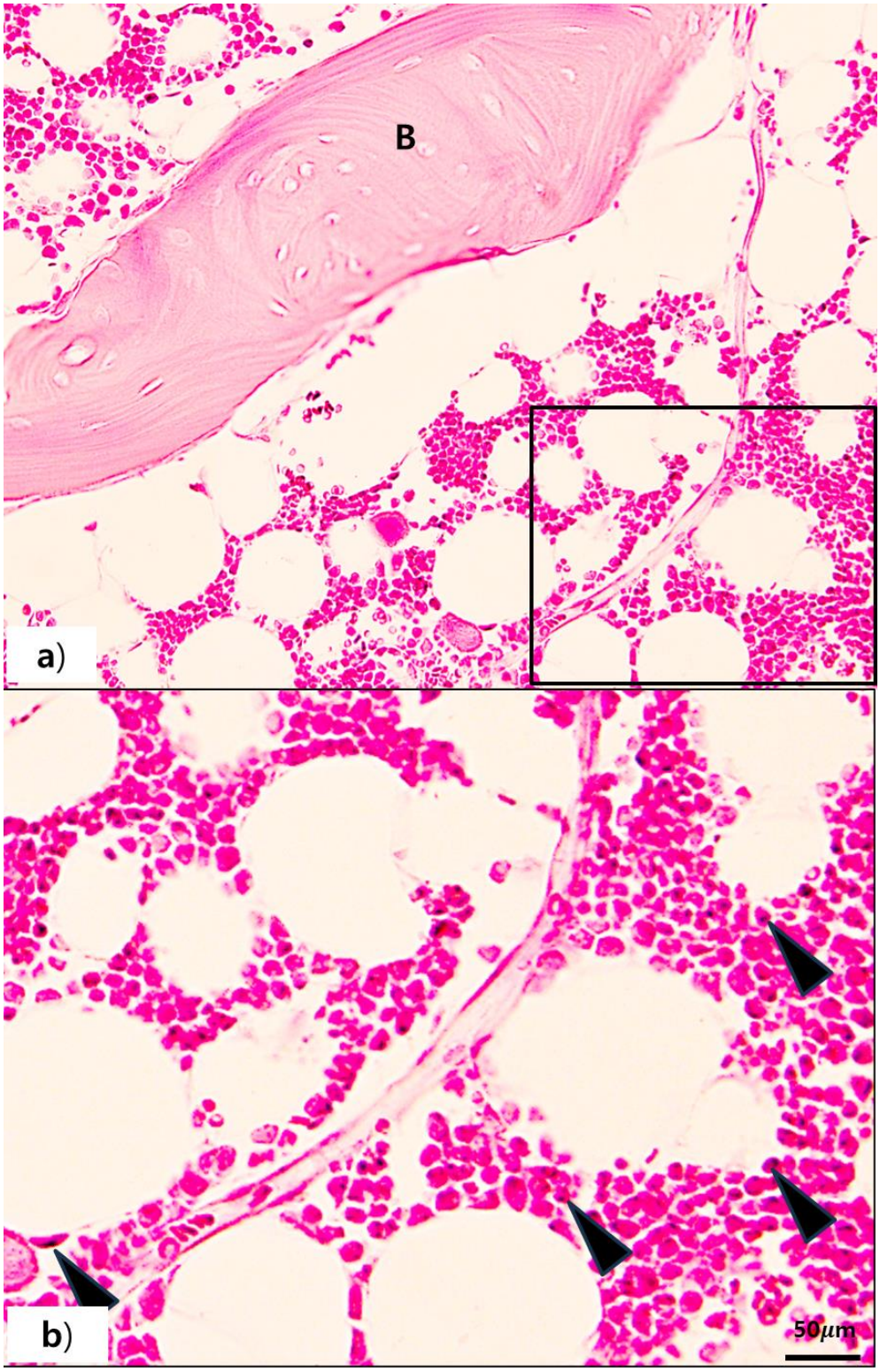

Figure 18. Histological features obtained through H&E staining in 3D scaffold.

The rectangles at the left (a) figures are magnified and represented at the right (b) figure. Black arrow: monocyte and neutrophil, B: bone

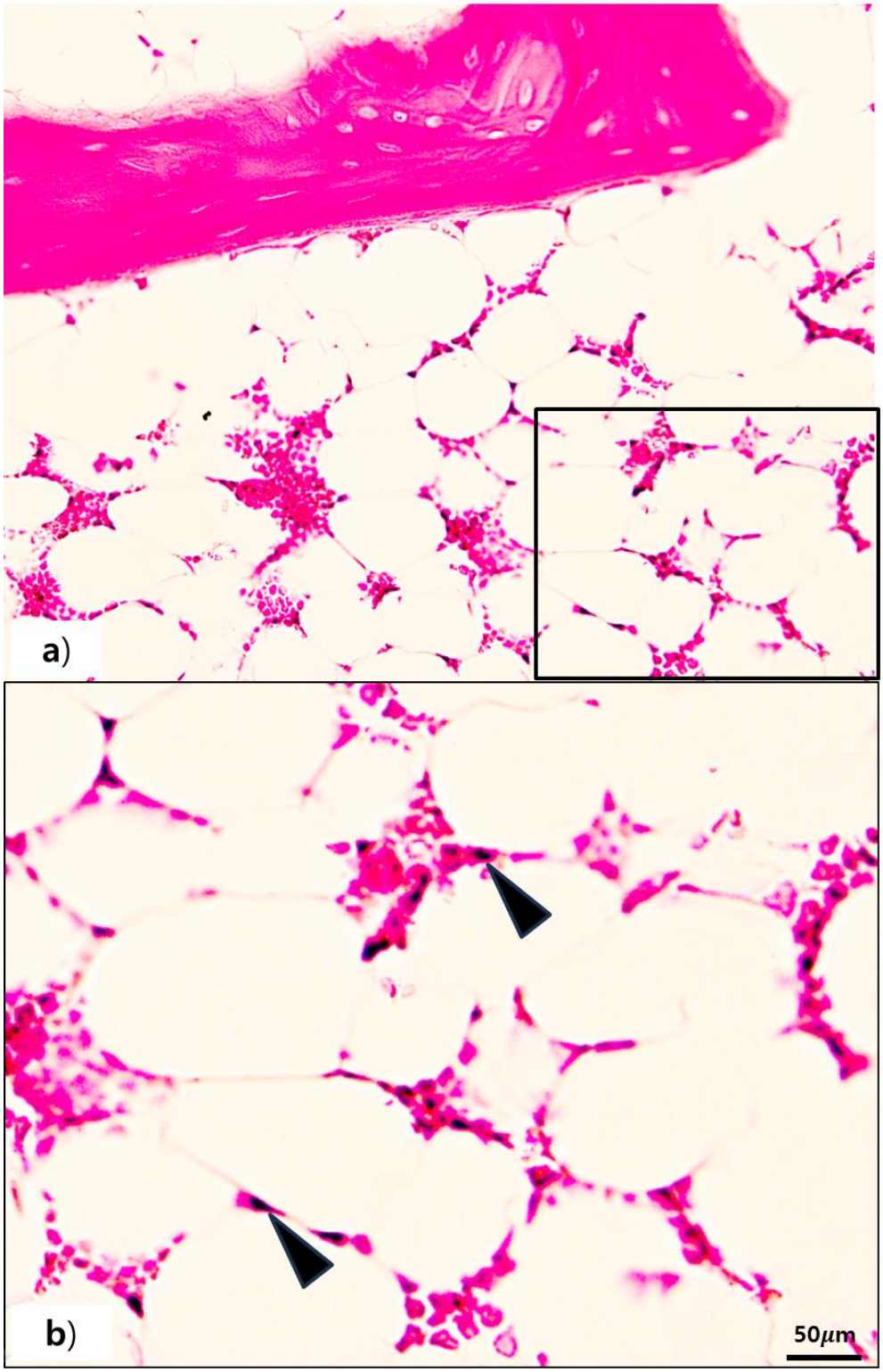

Figure 19. Histological features obtained through H&E staining in 4D scaffold.

The rectangles at the left (a) figures are magnified and represented at the right (b) figure. Black arrow: monocyte and neutrophil, B: bone

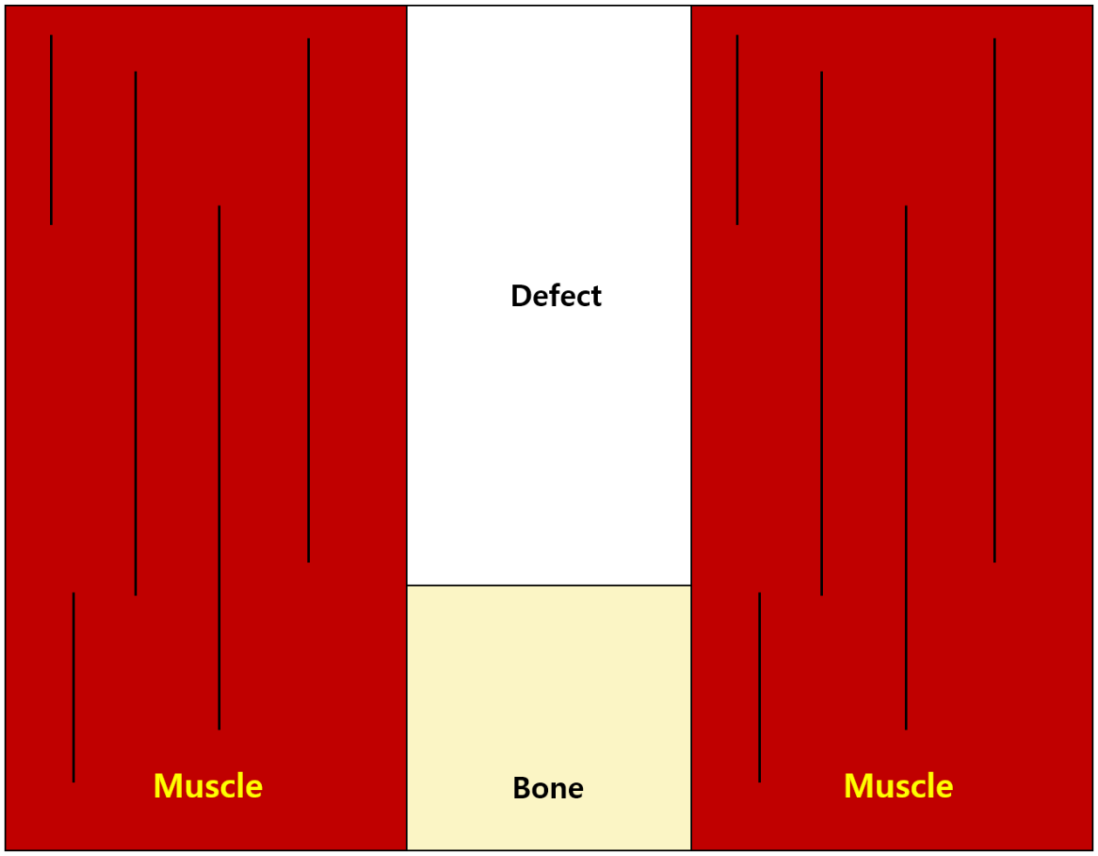

Figure 20. The relationship between the defect, bone, and muscles in the rabbit iliac crest model.

Muscles surrounding both lateral sides of the undercut area can exert pressure, potentially resulting in fractures and dislocation.

국문 요약

자가 맞춤형 4D 프린팅 기술을 활용한 토끼의 골 결손 부위에 이식된 골 이식재의 골 재생 력 평가

김민재

지도교수 이부규

울산대학교 대학원 의학과 치의학전공

개요

두개골 악안면부 영역에서는 종양, 낭 종, 외상, 골 괴사 등 다양한 원인으로 인해 골 결함이 발생할 수 있습니다. 따라서 골 결함으로 인한 장애를 해소하기 위해 재건이 필요합니다. 여러 결함 중에서는 좁은 입구로 구성된 undercut 형태의 골 결함이 흔히 관찰되며, 이러한 결함은 기존의 3D 프린팅 기술을 사용하여 재건하기 어렵습니다. 이 연구에서 사용된 맞춤형 4D 프린팅 기술의 이식 재료는 주변 수분을 흡수하고 팽창시키는 수화 겔의 특성을 이용하여 undercut 결함의 재건을 향상시켰습니다. 본 연구는 해당 4D 프린팅 골 이식 재료가 입체적 환경에서 두개골 악안면부 영역에 적합한지를 결정하는 것을 목표로 합니다.

재료 및 방법

총 16 마리 토끼가 사다리꼴 undercut 결함을 생성하고 결함 그룹, 3D 이식 재 그룹 및 4D 이식재 그룹으로 치료되었습니다. 6 주 및 12 주 후, 각 토끼가 희생되어 샘플이 준비되었습니다. 이후, CT 및 조직학적 분석을 통해 골 생성 능력, 팽창 능력 및 초기 구조의 유지 정도를 평가했습니다.

결과

연구에서는 골절(23%) 및 이식재 변위(23%)와 같은 다양한 합병증을 관찰했습니다. 정상적인 치유과정을 거친 사례에서 예상과 다르게 결손 부위에서 많은 골 재생이 일어났습니다. 하지만 이를 통해 이식재의 위치가 확인이 가능하여 골 생성 능력, 팽창 능력 및 초기 구조의 유지 정도를 평가할 수 있었습니다. 6 주에서 골 생성

분석 결과, 4D 이식재 그룹(29.16%)과 3D 이식 재 그룹(7.82%) 사이에 유의한 차이가 있었습니다. 4D 이식 재 그룹은 3D 이식 재 그룹보다 6 주에서 더 큰 음영 영역을 보여 4D 이식재의 팽창 능력을 확인했습니다. 또한 이식재의 초기 구조 유지 력을 평가하기 위해, 치유 전후로의 골 높이를 평가하였습니다. 그 결과, 4D 이식 재 그룹은 다른 그룹에 비해 초기 골 높이를 12 주에서 83%에서 87%로의 범위로 더 우수하게 유지했으며 3D 이식재와 비교 시 통계적으로 유의한 결과를 확인하였습니다. 조직병리학적 평가에서는 4D 이식 재 그룹에서 골 형성이 증가하고 염증 반응이 감소했습니다.

결론

이 연구는 두개골 악안면부 골 결함 재건을 위한 스카폴드 설계에 4D 프린팅 기술의 잠재력을 보여줍니다. 실험 모델에서는 두개골 악안면부 영역과는 다르게 골 형성 능력이 빠른 한계가 있었지만, 4D 지지대는 골 생성, 팽창 능력 및 구조의 유지 면에서 우수함을 확인할 수 있었습니다. 조직학적 검사는 4D 이식재의 생체 적합성 및 골 형성 능력을 확인했습니다. 더 많은 연구가 필요하지만, 이번 연구는 복잡한 골 결함을 해결하기 위한 4D 프린팅의 잠재력의 가능성을 보여줍니다.

중심어: 4D 프린팅 기술, 두개골 악안면부 재건, 골 결함